The Impact and Mitigation of Ionosphere Anomalies on Ground-Based Augmentation of GNSS

Sam Pullen, Young Shin Park, and Per Enge
Stanford University, Stanford, CA. USA

Abstract

This paper describes the impact that extreme ionospheric spatial gradients occurring during severe ionosphere storms have on GNSS Ground Based Augmentation Systems (GBAS) and how the U.S. Local Area Augmentation System (LAAS) mitigates the integrity risk due to these events. Gradients in slant ionosphere delay of as large as 425 mm/km over baselines of 40 – 100 km have been observed in CONUS during the ionosphere storms since April 2000 by both the U.S. Wide Area Augmentation System (WAAS) and the network of Continuously Operating Reference Station (CORS) reference receivers. Because ionosphere gradients affecting a LAAS site may not be observed by the LAAS Ground Facility (LGF) before users are affected, a simulation-based method has been developed to determine, in near-real-time, which potential LAAS user geometries would be unacceptably threatened by a hypothetical worst-case ionosphere gradient. Geometries of this type are made unavailable to LAAS users by having the LGF inflate the broadcast ionosphere-gradient sigma, which increases the Vertical Protection Level (VPL) of the unacceptable geometries so that they exceed the allowed Vertical Alert Limit (VAL).

1.0 Introduction

Ground Based Augmentation Systems (GBAS), such as the U.S. Local Area Augmentation System (LAAS), augment satellite navigation systems by providing differential corrections and integrity information to aviation users within several tens of kilometers of GBAS-equipped airports. Because the separation between GBAS reference stations and users is small and because GBAS corrections are updated twice per second, differential GBAS user errors due to typical spatial and temporal variations in ionosphere delay at L-band frequencies are almost negligible, even during solar-maximum conditions [1]. However, unusual ionosphere behavior during ionosphere storms observed by both the U.S. Wide Area Augmentation System (WAAS) and the network of Continuously Operating Reference Station (CORS) reference receivers has discovered spatial gradients in slant ionosphere delay of as large as 425 mm/km over baselines of 50 – 100 km. Gradients this large could cause vertical position errors for GBAS users of 20 meters or more if they coincide with poor user satellite geometry and the worst-case approach geometry and timing with respect to a single aircraft's approach to a specific GBAS-equipped airport.

This paper describes the procedure by which worst-case anomalous ionospheric spatial gradients are modeled, analyzed, and mitigated for GBAS. Section 2 identifies the largest ionosphere gradients discovered in WAAS and CORS data collected within the Conterminous U.S. (CONUS) since April of 2000. Section 3 briefly describes the data-analysis method used to examine past CORS data for large gradients, and Section 4 explains the simplified ionosphere anomaly "threat model" for LAAS use in CONUS generated from this data analysis. This threat model is combined with GPS and airport geometry simulations to predict the maximum differential range and position errors that LAAS users might suffer. A method for limiting these worst-case errors to acceptable levels by real-time broadcast integrity parameter inflation (to make "subset" satellite geometries that might lead to unacceptable errors unavailable to users) was developed and validated. Section 5 describes how this mitigation technique is implemented in the LAAS Ground Facility (LGF), the impact that this has on CAT I LAAS precision approach availability, and potential means to reduce the resulting availability loss by obtaining real-time ionosphere information from WAAS.

2.0 Severe Ionospheric Gradients Discovered in CONUS

Prior to 2002, it was believed that, during unusual ionosphere activity, ionospheric spatial gradients would not be more than 5 – 10 times greater than the value of 4 mm/km that was seen as a reasonable one-sigma bound on zenith ionosphere spatial gradients under both nominal and active ionosphere conditions, even during solar maximum (see [1]). However, WAAS data analysis of gradients that occurred in the Northeastern quadrant of the U.S. during the 6-7 April 2000 ionosphere storm showed gradients perhaps as large as 320 mm/km moving in a pattern similar to that of a weather front with varying speeds (see [2]). Gradients this large could not be bounded by any reasonable sigma value broadcast by a GBAS ground station, and they could generate vertical position errors for GBAS users that significantly exceed the 10-meter Vertical Alert Limit (VAL), or safe error bound, for GBAS-supported precision approaches to Category I weather minima [7].

A detailed search of known ionosphere storms in CONUS, using the method described in Section 3, discovered other examples of severe gradients. The most significant observed gradients were observed during the storm of 20 November 2003, which created a "filament" of greatly increased ionospheric delay over the Eastern half of CONUS, as shown in Figure 1. Very-large spatial gradients existed on both the leading (westward) and trailing (eastward) edges of this "finger" of enhanced delay, which moved in a roughly westward direction at an average speed of between 100 and 200 m/s (but with substantial local variation). Figure 2 shows the slant ionospheric delay from this event as observed by 7 CORS reference stations in Northern Ohio and Southern Michigan, where the largest spatial gradients were observed (see [3]). Note the rapid growth in delay associated with the passing of the leading edge of the "filament" in just under an hour, followed by a lengthy interval of erratic variation in ionospheric delay within the "filament" while the overall delay remains high, followed by a sudden, steep drop-off corresponding to the very sharp gradient corresponding to the trailing edge of the enhanced-delay feature. The largest gradient corresponding to this sharp depletion among the 7 stations shown in Figure 2 is about 330 mm/km, but another pair of CORS stations in Northern Ohio (ZOB1 and GARF) simultaneously observing GPS SVN 38 experienced a gradient of about 410 mm/km when the trailing edge passed, as shown in Figure 3.

While almost all extreme-gradient cases observed were for high-elevation satellites, a couple of cases existed where gradients as large as 360 mm/km were observed on low-elevation satellites, as shown by CORS stations WOOS and GARF tracking GPS SVN 26 on 20 November 2003, as shown in Figure 4. While, under normal conditions, the thin-shell model of the ionosphere suggests that slant ionospheric delay for low-elevation satellites would be as much as 3 times larger than that for satellites

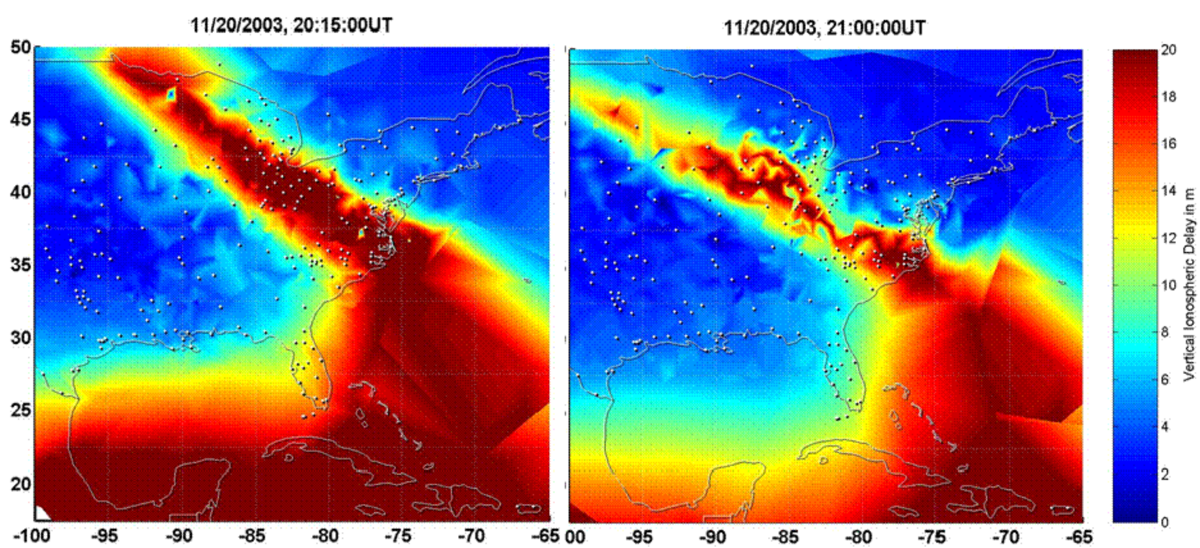

Figure 1: Enhanced Ionospheric Delay during 20 November 2003 Ionosphere Storm

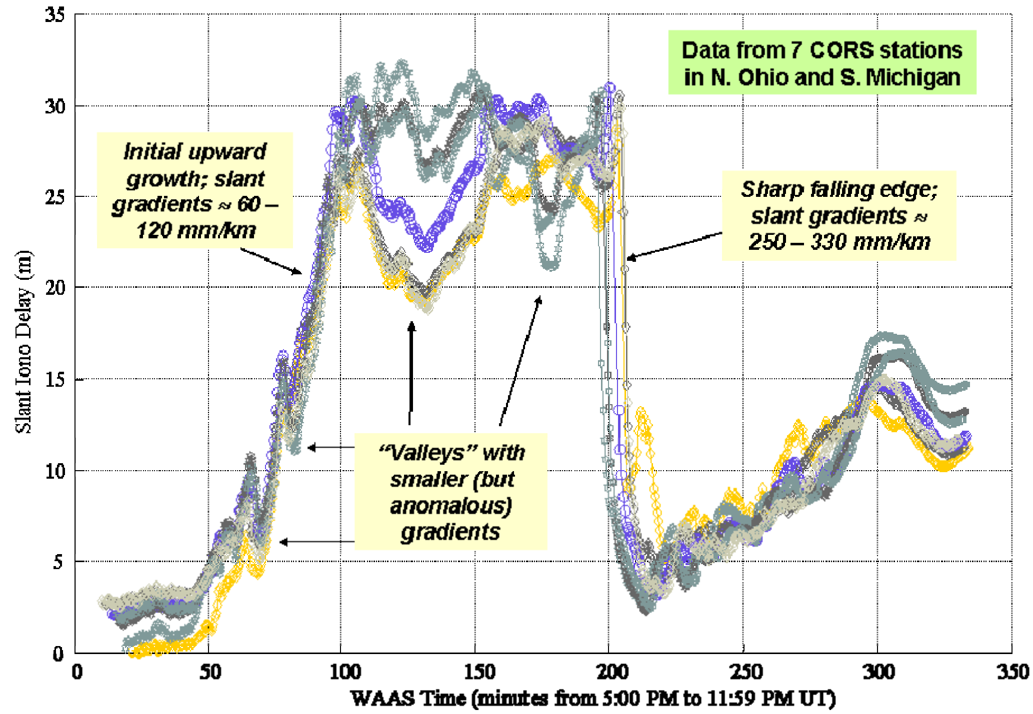

Figure 2: Ionospheric Delays at 7 CORS Stations during 20 November 2003 Ionosphere Storm

at zenith (90 degrees elevation), this model does not apply well to ionosphere storms, when it is thought that the bulk of the increased delay occurs at varied altitudes within the ionosphere (see [9]).

3.0 Ionosphere Storm Data Analysis Procedure

The largest gradients identified in Section 2 were the product of an exhaustive automated and manual analysis of all known ionosphere storm days in CONUS for which WAAS availability was affected (this would be due to the reaction of the WAAS ionosphere storm detector – see [10]). The details of this method are described in [3]. The primary data source for this analysis is both raw and post-processed CORS reference station data from hundreds of stations throughout CONUS. Ionospheric spatial gradients are calculated automatically for all satellites tracked by "clusters" of CORS stations within close proximity (several tens of kilometers) of each other in regions known to be affected by ionosphere storms. All apparent gradients of large anomalous magnitude (e.g., above 100 mm/km), calculated by dividing the difference in slant ionospheric delay between two CORS stations by the distance between the two stations, are put through a series of automated screening algorithms. These screening algorithms attempt to eliminate the most common non-ionospheric causes of apparent large gradients, which are CORS receiver "glitches" and errors in the CORS data-storage process [3]. CORS reference-station receivers are particularly vulnerable to semi-codeless tracking errors on L2 measurements during ionospheric anomalies, and these errors can make nominal or moderately-anomalous gradients seem much larger than they really are.

While the automated screening algorithms described in [3] greatly reduce the set of large spatial gradient events that are output by the data-analysis software, most of what remains is clearly due to CORS receiver or data-collection errors when manually examined by humans. Therefore, all significant events output by the software are reviewed by a group of humans who met regularly during the data-analysis process to examine the software results and determine if a significant, "verifiable" ionosphere-created gradient is present. If so, the best manual estimate of the resulting gradient was computed and added to the list of "valid" anomalous ionosphere events. The key to the manual-review process is a comparison between the apparent ionospheric gradient based on the post-processed

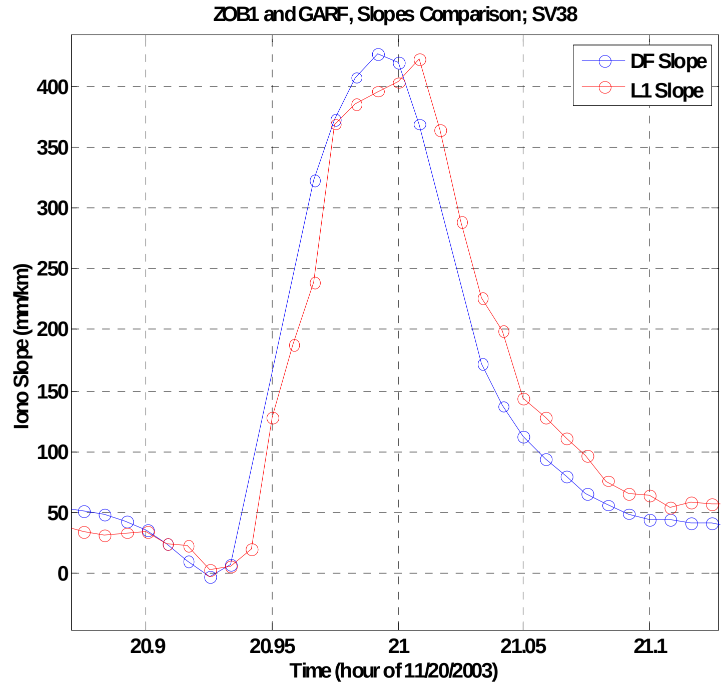

Figure 3: Gradient Observed Between ZOB1 and GARF on SVN 38, 20 November 2003

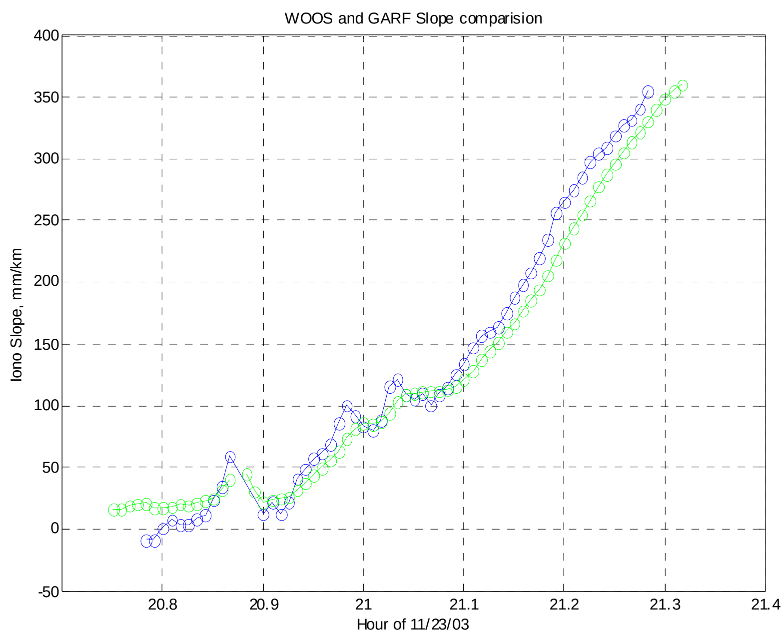

Figure 4: Gradient Observed Between WOOS and GARF on SVN 26, 20 November 2003

dual-frequency measurements and those based on code-minus-carrier measurements from the raw, single-frequency (L1-only) CORS measurements for the same stations and satellites (see [3]). As noted above, most receiver "glitches" affect the semi-codeless L2 measurements, and while post-processing removes most of these errors, the unusual measurement changes during ionospheric anomalies can introduce new errors. Figures 3 and 4 show two examples where large gradients reported by the data-analysis software (based on post-processed L1-L2 ionospheric-delay estimates) were validated by comparison with gradient estimates computed from raw L1 code-minus-carrier measurements from the same CORS receivers.

4.0 CONUS Ionosphere Anomaly Threat Model

Based on the largest validated ionospheric gradients reported in Section 2, Figures 5 and 6 show the resulting ionospheric spatial-gradient threat model for CONUS (also see [3,5,6]). Figure 5 shows the ionospheric-front geometry modeled in this threat model. The model assumes a linear change of ionospheric delay from high to low (or low to high) values, with the delay being constant on either side of the linear ramp. The front shown in Figure 5 is assumed to move with constant speed relative to the ground, and the other parameters of the front model (gradient and width) are assumed to also remain constant. It is known that these assumptions are not exactly true, but they serve as the most practical means of modeling the impact of a sharp ionosphere gradient on a GBAS or LAAS installation.

Figure 6 shows the upper bound on the maximum gradient of this threat model as a function of satellite elevation angle. These bounds slightly exceed the largest gradients validated from the data analysis due to margin added to account for measurement error. In addition to the plotted maximum gradient, bounds exist on speed with respect to the ground (up to 750 m/s), width (distance between high and low delay regions; between 25 and 200 km), and total differential delay (up to 50 meters) [3,6]. The differential-delay bound prevents combinations of gradient and width that separately would be within their respective bounds from being allowed if their product (the total differential delay) exceeds the bound, which is based on the maximum differential delay observed in data analysis [3].

Figure 7 shows the results of a simulation that characterizes "typical" impacts on GBAS users from an ionosphere anomaly posed by this threat model impacting two GPS satellites simultaneously for the LAAS facility at Memphis, Tennessee. Note that, for a LAAS user performing a CAT I precision approach in CONUS and reaching a 200-foot decision height 6 km from the centroid of the LGF reference antennas, the maximum differential pseudorange error generated by this threat model is 0.425 m/km × 20 km = 8.5 meters. The 20-km effective separation between LGF and user is the sum of 6 km of actual separation and 14 km of synthetic separation ($= 2\,\tau\, v_{air} \cong 2 \times 100\text{ s} \times 0.07\text{ km/s}$) due to the memory of the single-frequency carrier-smoothing filter (with τ = 100 sec) in the airborne receiver (see [4,11]). Figure 7 shows how pseudorange errors resulting from the range of allowed ionospheric front widths and velocities (only the largest and 2^{nd}-largest gradient sizes observed in the data analysis were used) and airborne positioning geometries combine to produce a range of vertical position errors. In about 75% percent of cases simulated, both affected GPS satellites are detected by the LGF CCD monitor before any differential error occurs, and in these cases, zeros are not entered

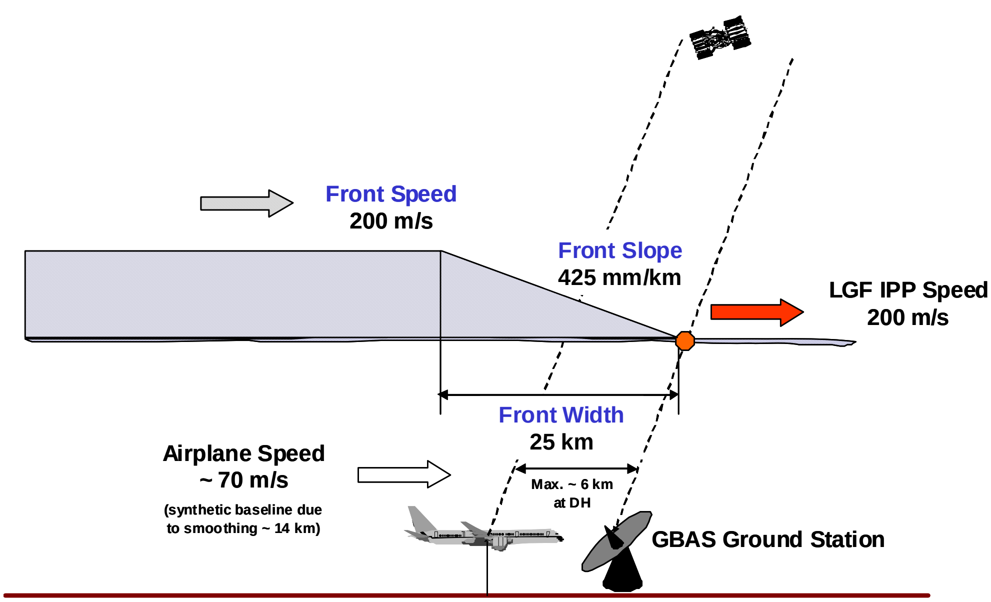

Figure 5: Ionosphere Threat Model Front Geometry

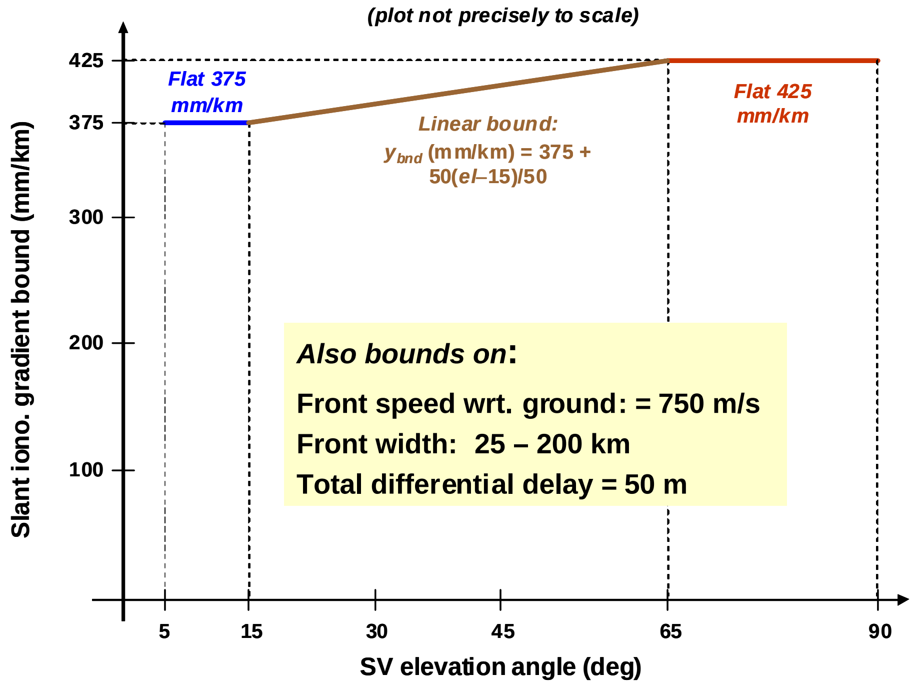

Figure 6: Ionosphere Threat Model Parameter Bounds

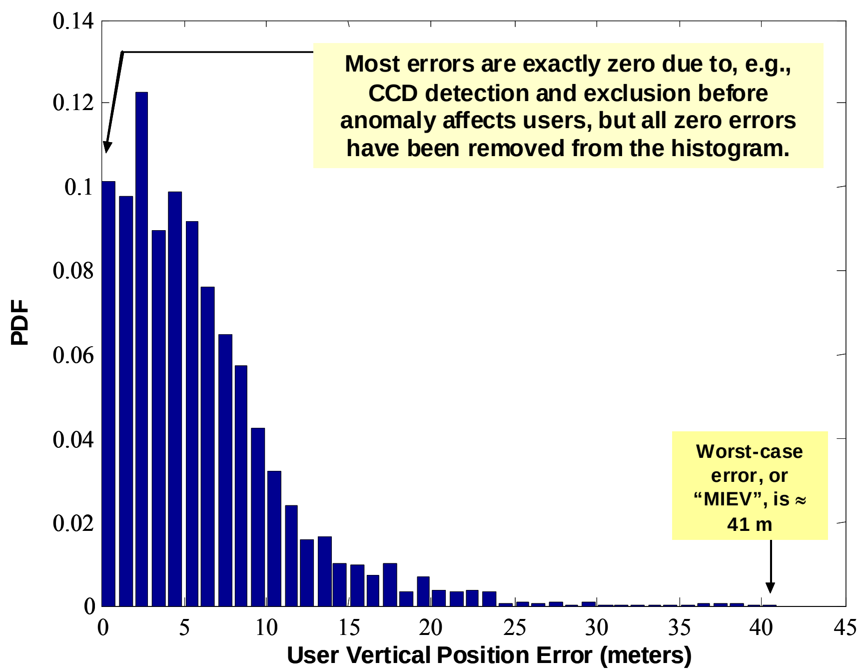

Figure 7: Typical "Near-Worst-Case" Anomaly-Induced Errors for GBAS Users

into the histograms. In most of the minority of cases shown in the histograms, the resulting non-zero vertical position error is small and non-threatening to precision-approach users, but in the very worst case, the error is as large as 41 meters. While the combination of worst-case events needed to generate errors of this magnitude would be extremely rare, even given a known ionosphere anomaly condition, this condition is deemed to be unsafe for CAT I precision approaches because this worst-case error magnitude exceeds an upper limit of 28.8 meters at the 200-foot decision height (DH) for a CAT I approach (see [8] for the derivation of this limit). Given that the worst-case scenario cannot be detected by the LGF, and the aircraft is not required to monitor for abnormal ionosphere rates-of-change, the only means of further mitigation of this risk is in the position domain, as described in the next section.

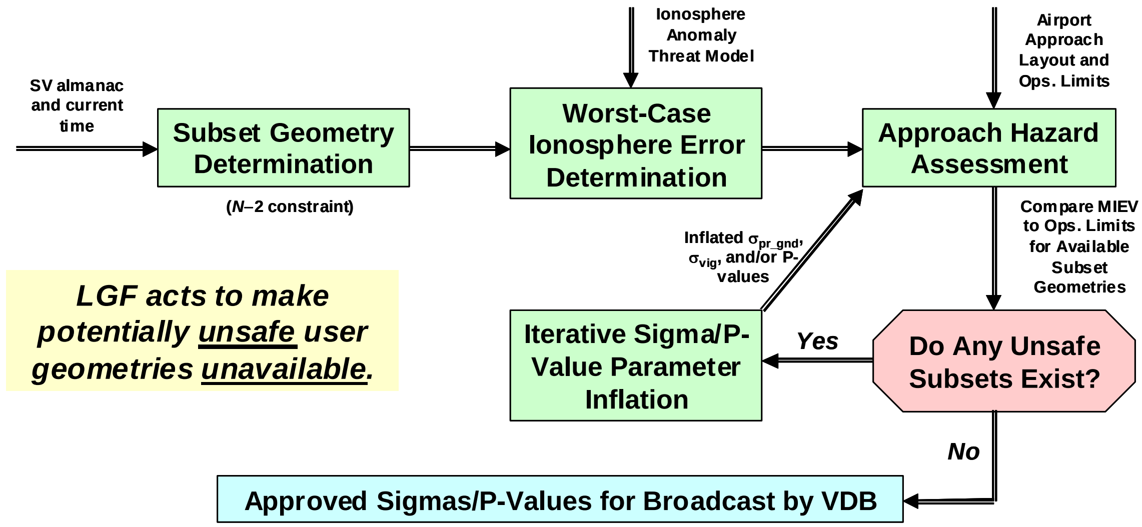

Figure 8: GBAS Ground System Geometry Screening Methodology Flow Diagram

5.0 Worst-Case Scenario Mitigation via Geometry Screening

Figure 8 shows a flow diagram of the methodology used by the LGF to protect users against unacceptable ionosphere-induced errors by restricting the set of GPS satellite geometries that are available to them (see [5,6]). The loop shown in Figure 8 is executed at regular intervals within the LGF processing (every 1 to 5 minutes, or every time a satellite rises into view or falls out of view). The first step is to enumerate all "credible" satellite geometries that aircraft approaching that LGF might make use of. In theory, any subset of 4 or more satellites of the set of *N* satellites for which corrections are broadcast can be used, but in practice, it is very unlikely that more than 2 of these *N* satellites will not be used (one complication involves airborne receivers with the minimum number of satellite-tracking channels allowed by the RTCA LAAS MOPS, which is 10 – see [12]). Based on this constraint, the LGF builds a list of all credible airborne geometries, determines which geometries from this subset could actually be used by the aircraft (meaning that they meet the VPL ≤ VAL requirement for CAT I precision approaches) and evaluates the worst-case ionosphere-induced vertical position error, or "MIEV", for each one at all CAT I DH locations supported by that LAAS site. Otherwise-usable geometries for which the MIEV exceeds the safe error limit of 28.8 meters at any DH location must be made unavailable so as not to threaten users, and this is done by increasing one or more of the broadcast sigma or P-values that help determine VPL such that VPL for all "unsafe" geometries exceeds VAL and makes all such geometries unavailable (see [12]). An optimized method for doing this based on inflation of both σ_{pr_gnd} and P-values for each individual satellite is given in [6]. A simpler method of inflating only the single σ_{vig} value that covers all satellites is given in [5].

While sigma and/or P-value inflation is required to eliminate "unsafe" geometries, it has the unavoidable impact of making "safe" geometries unavailable as well. As a result, the achievable CAT I system availability with geometry screening included is significantly lower than what it would be if geometry screening were not required. However, most major airport locations in CONUS will still achieve CAT I availabilities of 0.999 or better when all 24 GPS satellites in primary orbit slots are functioning and healthy. Note that this penalty is suffered because the threat model in Section 4 is presumed to be present at all times. The best way to reduce this penalty is to remove this conservative assumption, and the most practical means to do so at present is to receive Wide Area Augmentation System (WAAS) ionosphere corrections and GIVE values at LAAS sites. When WAAS GIVE values indicate that no ionosphere storms are affecting a given satellite being tracked by the LGF, that LAAS site can be assured that the satellite in question has no risk of being affected by a threatening ionosphere gradient, and geometry screening is not needed for that satellite (see [13]).

Acknowledgments

The authors would like to thank Ming Luo, Jiyun Lee, Seebany Datta-Barua, Shankar Ramakrishnan, Godwin Zhang, Todd Walter, and Juan Blanch at Stanford, Mats Brenner and Kim Class at Honeywell, and John Warburton, Barbara Clark, Hamza Abdusalem, and Jason Burns of the FAA. We would also like to thank Attila Komjathy of the Jet Propulsion Laboratory for performing the post-processing of dual-frequency CORS reference station data. This research was funded by the FAA Satellite Navigation LAAS Program Office, and the support of Leo Eldredge, Carlos Rodriguez, and Ted Urda is greatly appreciated. However, the opinions expressed in this paper are solely those of the authors and do not necessarily represent those of the FAA.

References

[1] Lee, J., S. Pullen, S. Datta-Barua, and P. Enge, "Assessment of Ionosphere Spatial Decorrelation for Global Positioning System-Based Aircraft Landing Systems", *AIAA Journal of Aircraft*, Vol. 44, No. 5, Sept.-Oct. 2007, pp. 1662-1669. http://www.aiaa.org

[2] S. Datta-Barua, T. Walter, S. Pullen, M. Luo, J. Blanch, and P. Enge. "Using WAAS Ionospheric Data to Estimate LAAS Short Baseline Gradients," *Proceedings of ION 2002 National Technical Meeting*, San Diego, CA, Jan. 28-30, 2002, pp. 523-530. http://waas.stanford.edu/~wwu/papers/gps/PDF/DattaBaruaIONNTM02.pdf

[3] A. Ene, D. Qiu, M. Luo, S. Pullen, and P. Enge, "A Comprehensive Ionosphere Storm Data Analysis Method to Support LAAS Threat Model Development," *Proceedings of ION 2005 National Technical Meeting*, San Diego, CA, Jan. 24-26, 2005, pp. 110-130. http://waas.stanford.edu/~wwu/papers/gps/PDF/EneQiuIONNTM05.pdf

[4] D. V. Simili and B. Pervan, "Code-Carrier Divergence Monitoring for the GPS Local Area Augmentation System, *Proceedings of IEEE/ION PLANS 2006*, San Diego, CA, April 25-27, 2006, pp. 483-493. http://www.ion.org/search/view_abstract.cfm?jp=p&idno=6677

[5] J. Lee, M. Luo, S. Pullen, Y. S. Park, P. Enge, and M. Brenner, "Position-Domain Geometry Screening to Maximize LAAS Availability in the Presence of Ionosphere Anomalies," *Proceedings of ION GNSS 2006*, Fort Worth, TX, Sept. 26-29, 2006. http://waas.stanford.edu/~wwu/papers/gps/PDF/LeeIONGNSS06.pdf

[6] S. Ramakrishnan, J. Lee, S. Pullen, and P. Enge, "Targeted Ephemeris Decorrelation Parameter Inflation for Improved LAAS Availability during Severe Ionosphere Anomalies," *Proceedings of ION 2008 National Technical Meeting*, San Diego, CA, Jan. 28-30, 2008, pp. 354-366. http://waas.stanford.edu/~wwu/papers/gps/PDF/RamakrishnanIONNTM08.pdf

[7] *Minimum Aviation System Performance Standards for Local Area Augmentation System (LAAS)*. Washington, D.C., RTCA SC-159, WG-4, DO-245A, Dec. 9, 2004. http://www.rtca.org

[8] C.A. Shively and R. Niles, "Safety Concepts for Mitigation of Ionospheric Anomaly Errors in GBAS," *Proceedings of ION 2008 National Technical Meeting*, San Diego, CA, Jan. 28-30, 2008, pp. 367-376. http://www.ion.org/search/view_abstract.cfm?jp=p&idno=7695

[9] S. Datta-Barua, T. Walter, S. Pullen, and P. Enge, "Modeling the 20 November 2003 Ionosphere Storm with GRACE," *Proceedings of ION GNSS 2007*, Fort Worth, TX, Sept. 25-28, 2007, pp. 2840-2848. http://waas.stanford.edu/~wwu/papers/gps/PDF/DattaBaruaIONGNSS07.pdf

[10] T. Walter, A. Hansen, J. Blanch, *et al*, "Robust Detection of Ionospheric Irregularities," *Proceedings of ION GPS 2000*, Salt Lake City, UT, Sept. 19-22, 2000, pp. 209-218. http://waas.stanford.edu/~wwu/papers/gps/PDF/toddion00.pdf

[11] P.Y. Ko, *GPS-Based Precision Approach and Landing Navigation: Emphasis on Inertial and Pseudolite Augmentation and Differential Ionosphere Effect*, Ph.D. Dissertation, Stanford University, Department of Aeronautics and Astronautics, May 2000. http://waas.stanford.edu/~wwu/papers/gps/PDF/Thesis/PingYaKoThesis00.pdf

[12] *Minimum Operational Performance Standards for GPS Local Area Augmentation System Airborne Equipment*. Washington, D.C., RTCA SC-159, WG-4, DO-253B, June 26, 2007. http://www.rtca.org

[13] S. Pullen, M. Luo, T. Walter, and J. Blanch, "Proposed Algorithm for LAAS use of WAAS for Ionosphere Threat Determination," Honeywell LAAS Technical Interchange Meeting #12, Coon Rapids, MN, Dec. 8, 2004. http://waas.stanford.edu